A novel analytical solution for ponded infiltration with consideration of a developing saturated zone

DongHao Ma[1#], ZhiPeng Liu[2#], SiCong Wu[1, 3], and JiaBao Zhang[1]

[1] State Experimental Station of Agro-Ecosystem in Fengqiu, State Key Laboratory of Soil and Sustainable Agriculture, Institute of Soil Science, Chinese Academy of Sciences, Nanjing 210008, China.

[2] College of Resources and Environmental Sciences, Nanjing Agricultural University, Nanjing 210095, China.

[3] University of Chinese Academy of Sciences, Beijing 100049, China.

[3] University of Chinese Academy of Sciences, Beijing 100049, China.

[#] These authors contributed equally to this work.

Corresponding author: JiaBao Zhang (jbzhang@issas.ac.cn)

Key Points:

- The saturated zone is longer than the unsaturated wetted zone during ponded infiltration.
- The new proposed infiltration equation includes an expression of the saturation zone versus time.
- The new solution simulates infiltration and estimates soil hydraulic properties more accurately.

Abstract

Ponding at the soil surface exerts profound impacts on infiltration. However, the effects of ponding depth on infiltration, especially the development of a saturated zone below the soil surface, have not been considered in present infiltration models. A new general Green-Ampt model solution (GAMS) was derived for a one-dimensional vertical infiltration into soils under a uniform initial moisture distribution with ponding on its surface. An expression was included in the new solution for simulating the saturated layer developed below the soil surface as long as the pressure head at the surface is greater than the water-entry suction. The GAMS simulates the infiltration processes closer to the numerical solution by HYDRUS-1D than the traditional and a recently improved Green-Ampt model. Moreover, an inversion method to improve the estimates of soil hydraulic parameters from one-dimensional vertical infiltration experiments that is based on the GAMS was suggested. The effect of ponding depth (h_p), initial soil moisture content, soil texture, and hydraulic soil properties (K_s, h_d and n) in the saturated zone was also evaluated. The results indicate that the saturated zone developed at a much faster rate than the unsaturated zone during infiltration. Generally, a larger saturated zone was found for soils with higher initial soil moisture content, coarser texture, higher K_s values and lower h_d and n. Our findings reveal that including the saturated zone in the infiltration model yields a better estimate for the soil hydraulic parameters. The proposed GAMS model can improve irrigation design and rainfall-runoff simulations.

1 Introduction

Infiltration is one of the most important components of land surface water cycles. Accurate simulation of infiltration rate is crucial in hydrological forecast, biogeochemical process simulation, agricultural water management, and soil and water conversation (Assouline, 2013).

However, infiltration is a complex process affected by many factors such as (1) soil structure and its spatial heterogeneity influenced by soil mineral particles and organic matter in physical, chemical and biological cycles (Bonetti et al., 2021; Fatichi et al., 2020; Vereecken et al., 2022); (2) chemical compositions of the soil water and infiltrating water (Klopp and Daigh, 2020); (3) initial soil moisture distribution across soil profile (Stewart et al., 2013; Wu et al., 2021); (4) type and rate of water supply on the soil surface (Assouline et al., 2007; Corradini et al., 1994; 1997). During the past one century, a vast amount of attentions have been attracted to the studies on developing mathematical infiltration models under various conditions (Green and Ampt, 1911; Haverkamp et al., 1994; Hogarth et al., 2013; Morbidelli et al., 2018; Moret-Fernández et al., 2020; Parlange, 1971; Parlange et al., 1982; Philip, 1969; Selker and Assouline, 2017; Stewart, 2019; Talsma and Parlange, 1972), as well as establishing methods to determine infiltration model parameters (Angulo-Jaramillo et al., 2019; Ma et al., 2017; Neuman, 1976; Parlange, 1975; Touma et al., 2007; Valiantzas, 2010; Vauclin and Haverkamp, 1985). Generally, the model expression and its deriving method for one-dimentional infiltration into homogeneous soils with uniform initial soil moisture distributions under a saturated or ponded upper boundary condition were taken as a base for the development of one, two or three-dimentional infiltration models under more complex conditions (Kargas and Londra, 2021; Selker and Assouline, 2017; Wu et al., 2022).

The effects of ponding on infiltration can be profound (Philip, 1958a; 1958b), especially in initially wet soils, and it acts through not only added surface water pressure but also water redistribution in soils (Parlange, 1972). The ponding can increase water pressure at soil surface and thus improve infiltration. Soil moisture profile would change accordingly to transmit and redistribute soil water potential gradient across the whole profile. Consequently, a saturated zone

forms below the soil surface and increases during ponded infiltration. In addition, for soils with non-zero water-entry suction ($-h_d$), the saturated zone, defined as tension-saturated zone by (Philip, 1958a), would still develop even if the surface water pressure is zero or a negative value greater than water-entry suction (Haverkamp et al., 1990). Given that soils with non-zero water-entry suction are common in nature, a saturated zone composed of the two types above was found in most soil moisture profiles during infiltration under a surface pressure greater than water-entry suction (Philip, 1958a).

However, the effects of ponded water on infiltration have not been fully considered in the two types of widely used infiltration models under ponded conditions. One type includes the empirical and semi-empirical models which neglect the effect of ponding depth, such as Horton's infiltration model (Horton, 1941) in hydrology, Kostiakov model (Kostiakov, 1932) and Lewis-Kostiakov model (Mezencev, 1948) in surface irrigation. The other type includes analytical and semi-analytical infiltration models, such as Philip's Two-Term model (Philip, 1957a), Brutsaert's model (Brutsaert, 1977), Parlange's three-parameter model (Parlange et al., 1982), Swartzendruber model (Swartzendruber, 1987), the traditional Green-Ampt model (TGAM) (Green and Ampt, 1911) and the recently improved Green-Ampt model (GAME) (Ma et al., 2015). In these analytical and semi-analytical models, the effects of ponding depth on infiltration were only expressed in the form of an added surface pressure head.

Actually in 1958, Philip (1958a) has proposed an analytical method which includes a series expression of the time-dependent saturated zone by assuming a negligible effect of ponding depth on infiltration rate. His solution showed a good simulation accuracy in a short time and revealed a time-dependent soil moisture profile shape (Philip, 1958b). In 1972, Parlange (1972) built a general iterative solution in integral forms addressing the infiltration under ponded

conditions, which can achieve accurate simulation for a longer time. A more concise solution was derived by Haverkamp et al. (1990) to depict the effects of ponding depth on infiltration, based on the first-order approximation of the above Parlange's solution (Parlange, 1972) and a flux-saturation relation. These solutions substantially improved the infiltration simulation by taking into account the profound effects of ponding depth on infiltration. Unfortunately, few of the results has been adopted in subsequent infiltration simulations. One of the most important reasons is that the solutions in integral forms are too complex to use in practice.

The main applications of infiltration formulas are to simulate infiltration and to estimate its parameters. During the past two decades, some analytical or semi-analytical solutions to infiltration problems have found their exciting function of rapidly inverting soil hydraulic properties from infiltration experiments (Jaiswal et al., 2022; Ma et al., 2016, 2017; Rahmati et al., 2021) and overcoming the problem of non-convergence and unitability in numerical inversion. However, the accuracy of the inverted parameters of soil hydraulic property model were found sensitive to the accuracy of the forward analytical or semi-analytical solutions (Ma et al., 2009). A small difference in an infiltration formula from a real infiltration process may result in time-dependent estimated parameters in its applications. Our previous studies (Ma et al., 2015, 2017) exhibited that to build the quantitative relationship between the Green-Ampt model simple in form and Richards equation accurate in simulation was an effective approach to achieve soil hydraulic properties from infiltration experiments. The traditional Green-Ampt model (TGAM) is just a special solution to Richards equation for soils with delta-type diffusivity (Philip, 1957b) and thus too simplified to accurately estimate soil hydraulic properties. Recently, a more sophisticated Green-Ampt model (GAME) found its deterministic relevance to Richards equation for general soils (Ma et al., 2015). Based on the new approximate analytical solution, a

compatible method was derived to determine soil hydraulic properties (Ma et al., 2015, 2017). However, the effects of ponding depth on infiltration were still not fully considered in that solution, especially the changes in the shape of soil moisture profile.

Therefore, the objectives of this research are (1) to develop a new solution to one-dimensional infiltration under ponded conditions, including a simple infiltration equation with ponding depth effects and explicit expressions of saturated and unsaturated zone length varying with time; (2) to evaluate the effects of ponding depth on infiltration simulation and soil hydraulic parameter estimation.

2 Theory

2.1 A general solution to infiltration with a constant water head

According to Ma et al. (2015), a general relationship for a vertical infiltration into soils with initially uniform soil moisture distribution under ponding with a constant water depth is given as:

$$\int_0^{z_f}\left(\left(J_{w0}-K_i\right)F+K_i\right)dz=\int_0^{z_f}Kdz-\int_0^{h_i}Kdh-\int_{h_p}^{0}Kdh \qquad (1)$$

where K is the soil hydraulic conductivity (cm min^{-1}); K_i is the soil hydraulic conductivity at the initial soil water content (cm min^{-1}); J_{w0} is the infiltration rate or surface soil water flux (cm min^{-1}); F is the soil water flux-saturation function; h is the soil water pressure head (cm); h_i is the initial soil water pressure head (cm); h_p is the water depth on soil surface (cm); z is the soil depth (cm) with zero point at soil surface and downward coordinate axis; and z_f is the wetting front advance or the length of wetted zone (cm).

Since J_{w0} is a variable independent of z, after rearranging Equation (1), it is expressed as:

$$J_{w0} = \frac{\int_0^{z_f} \left(K - (1-F) K_i\right) dz - \int_0^{h_i} K dh - \int_{h_p}^{0} K dh}{\int_0^{z_f} F dz} \quad (2)$$

Since the saturated soil drains only when water head drops below air entry suction $-h_d$ (cm), there must be a saturated zone on the upper part of the wetted zone where $h > -h_d$. Assuming that soil water content profile in the unsaturated wetted zone can be described with a simple function (e.g. in Ma et al., 2015) and its relative shape does not change with time, then the soil water content profile (Figure 1) can be described as:

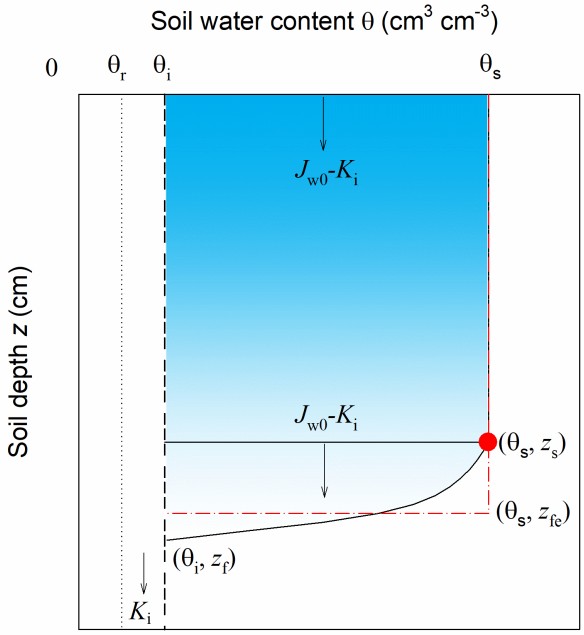

Figure 1. Schematic diagram of soil moisture profile including saturated and unsaturated wetted zones. θ_r and θ_i are the residual and initial soil water content, respectively; θ_s is the soil water content at the water inlet; J_{w0} is the surface water flux; K_i is the soil hydraulic conductivity at θ_i; z_s is the length of saturated zone; z_f and z_{fe} are actual and equivalent lengths of wetted zone, respectively.

$$S = \frac{\theta - \theta_r}{\theta_s - \theta_r} = \begin{cases} 1 & z < z_s \\ S\left(\dfrac{z - z_s}{z_f - z_s}\right) & z_f \geq z \geq z_s \\ S_i & z \geq z_f \end{cases} \quad (3)$$

where θ is the soil water content ($cm^3\ cm^{-3}$); θ_s and θ_r are the saturated and residual soil water content ($cm^3\ cm^{-3}$), respectively; S is the relative saturation; S_i is the relative saturation at, θ_i, the initial soil water content ($cm^3\ cm^{-3}$); z_s is the length of saturated zone (cm).

Correspondingly, the soil hydraulic conductivity in the profile is written as

$$K = \begin{cases} K_s & 0 \leq z < z_s \quad h > -h_d \\ K(h) & z_f \geq z \geq z_s \quad h_i \leq h \leq -h_d \\ K_i & z \geq z_f \quad h = h_i \end{cases} \quad (4)$$

where K_s is the saturated soil hydraulic conductivity ($cm\ min^{-1}$).

Then, with Equation (4), the second and third terms on the right side of Equation (1) can be transformed to

$$\int_0^{h_i} K dh = \int_{-h_d}^{h_i} K dh + \int_0^{-h_d} K dh = \int_{-h_d}^{h_i} K dh - K_s h_d \quad (5)$$

$$\int_{h_p}^{0} K dh = -K_s h_p \quad (6)$$

According to Philip (1973), the relationship between F and soil water content can be described with a simple function:

$$F(\theta) = \frac{J_w - K_i}{J_{w0} - K_i} = \frac{\theta - \theta_i}{\theta_s - \theta_i} \quad (7)$$

where J_w is the soil water flux (cm min^{-1}). More accurate functions can be found in Ma et al. (2017a). No matter what the specific function of F is, F should be 1 in the saturated zone and gradually decreases from 1 to 0 in the unsaturated wetted zone.

Defining the equivalent wetting front length of the unsaturated wetted zone (Figure 1) as z_{ufe} by using the piston-type assumption of water flow in Green & Ampt (1911), after considering Equation (3) and Equation (7), we get

$$z_{ufe} = \frac{\int_{z_s}^{z_f} (\theta - \theta_i) dz}{\theta_s - \theta_i} = (z_f - z_s) B_0 \tag{8}$$

where

$$B_0 = \int_0^1 \frac{\theta - \theta_i}{\theta_s - \theta_i} d \frac{z - z_s}{z_f - z_s} \tag{9}$$

Combining Equation with Equation (8) yields

$$\int_0^{z_f} F dz = z_s + \int_{z_s}^{z_f} F dz = z_s + z_{ufe} \tag{10}$$

$$\int_0^{z_f} \left(K - (1-F) K_i\right) dz = K_s z_s + \frac{z_{ufe}}{B_0} \int_0^1 \left(K - (1-F) K_i\right) d \frac{z - z_s}{z_f - z_s} \tag{11}$$

Substituting Equation (5), Equation (6), Equation (10) and Equation (11) in Equation (2) and rearranging the equation, the expression of J_{w0} related to the length of saturated zone and the equivalent one of unsaturated wetted zone can be expressed as

$$J_{w0} = K_s \left(1 + \frac{B_1 + B_3 - B_2 z_{ufe}}{z_s + z_{ufe}}\right) \tag{12}$$

where

178
$$B_1 = -\int_{-h_d}^{h_i} \frac{K}{K_s} dh \tag{13}$$

179
$$B_2 = 1 - \frac{\int_0^1 \left(\frac{K}{K_s} - (1-F)\frac{K_i}{K_s} \right) d\frac{z - z_s}{z_f - z_s}}{\int_0^1 F d\frac{z - z_s}{z_f - z_s}} \tag{14}$$

180
$$B_3 = h_p + h_d \tag{15}$$

181 Actually, the expression of J_{w0} can be also derived by applying Darcy's law to the saturated
182 zone. Soil water flux is evenly distributed with saturated hydraulic conductivity in the saturated
183 zone. The pressure head should be h_p at the upper boundary of the saturated zone and -h_d at its
184 bottom.

185 Then,

186
$$J_{w0} = K_s \left(1 + \frac{h_p + h_d}{z_s} \right) = K_s \left(1 + \frac{B_3}{z_s} \right) \tag{16}$$

187 Combining Equation (12) with Equation (16) yields

188
$$z_{ufe} = \frac{B_1 z_s}{B_2 z_s + B_3} \tag{17}$$

189 According to the definition by Green and Ampt (1911), the length of equivalent wetted zone, z_{fe},
190 should be the sum of the saturated zone length, z_s, and the equivalent wetting front length of the
191 unsaturated zone, z_{ufe}, that is,

192
$$z_{fe} = z_s + z_{ufe} = z_s + \frac{B_1 z_s}{B_2 z_s + B_3} \tag{18}$$

193 Then,

194 $$I=\left(\theta_s-\theta_i\right)z_{fe}+K_i t=\left(\theta_s-\theta_i\right)\left(z_s+\frac{B_1 z_s}{B_2 z_s+B_3}\right)+K_i t \tag{19}$$

195 where I is the cumulative infiltration or cumulative surface water flux (cm); K_i is normally
196 negligible in most cases.

197 Since the surface water flux is the derivative of the cumulative infiltration, we obtain other
198 expression of J_{w0} by neglecting K_i,

199 $$J_{w0}=\frac{dI}{dt}=\left(\theta_s-\theta_i\right)\frac{dz_{fe}}{dt}=\left(\theta_s-\theta_i\right)\left(1+\frac{B_1 B_3}{\left(B_2 z_s+B_3\right)^2}\right)\frac{dz_s}{dt} \tag{20}$$

200 Combining Equation (16) and Equation (20) to eliminate J_{w0} and conducting definite
201 integration of z_s from 0 to z_s and t from 0 to t, we derive the implicit expression of the saturated
202 zone length with time,

203 $$z_s-\left(B_3+B_5\right)\ln\left(1+\frac{z_s}{B_3}\right)+B_5\ln\left(1+\frac{B_2 z_s}{B_3}\right)+\frac{B_1}{\left(1-B_2\right)B_2}\left(1-\frac{B_3}{\left(B_2 z_s+B_3\right)}\right)=B_4 t \tag{21}$$

204 where

205 $$B_4=\frac{K_s}{\theta_s-\theta_i} \tag{22}$$

206 $$B_5=\frac{B_1}{\left(1-B_2\right)^2} \tag{23}$$

207 With Equation (8) and Equation (17), z_f can be derived from z_s

208 $$z_f=z_s+\frac{1}{B_0}z_{ufe}=z_s+\frac{B_1 z_s}{B_0\left(B_2 z_s+B_3\right)} \tag{24}$$

Given flux–saturation relationship F, specific soil moisture profile function (S~z), soil hydraulic properties (K~h and h~θ), initial condition (θ_i) and boundary condition (h_p), the length of saturated zone can be calculated by solving Equation (21). Then, the cumulative infiltration can be calculated from z_s by using Equation (19). Accordingly, the surface water flux and the length of the wetted zone can be calculated using Equation (16) and Equation (24), respectively. Finally, Equation (16), Equation (19), Equation (21) and Equation (24) constitute a new solution to one-dimensional vertical infiltration with the upper boundary of a constant pressure head. In order to differentiate the new solution from TGAM and GAME, the new solution is named as Green-Ampt Model Solution, the GAMS.

2.2 A special solution for infiltration with Brooks-Corey model

Soil water retention curves and unsaturated hydraulic conductivities can be described using the model proposed by Brooks and Corey (1964), denoted as the BC model:

$$S(h)=\begin{cases}\dfrac{\theta-\theta_r}{\theta_s-\theta_r}=\left|\dfrac{h_d}{h}\right|^n & h<-h_d \\ 1 & h\geq -h_d\end{cases} \tag{25}$$

$$K(h)=\begin{cases}K_s\left|\dfrac{h_d}{h}\right|^m=K_sS^{m/n} & h<-h_d \\ K_s & h\geq -h_d\end{cases} \tag{26}$$

where $m = (l + 1)\, n + 2$ with Burdine's method (Burdine, 1953); l is the soil pore tortuosity factor and normally $l = 2$ in the BC model.

With the upper boundary condition of saturation (i.e. $h = - h_d$), Ma et al. (2015) derived an expression of soil moisture profile for infiltration into soils with initially uniform soil water content. Similar expression can be obtained with exactly the same deriving steps in Ma et al.

228 (2015) for the soil water content profile of the unsaturated wetted zone in the current study.
229 Substituting the length of unsaturated zone here for the length of wetted zone in Ma et al. (2015)
230 yields,

231 $$S = \left(1 - b\frac{z - z_s}{z_f - z_s}\right)^a \tag{27}$$

232 where

233 $$a = \frac{n}{2n+2} \tag{28}$$

234 $$b = 1 - S_i^{1/a} \tag{29}$$

235 Substituting Equation (25)-(27) to Equation (13) and Equation (14), we get

236 $$B_0 = (\theta_s - \theta_r)\frac{1-(1+ab)S_i}{b(a+1)} \tag{30}$$

237 $$B_1 = \frac{1-S_i^{3+1/n}}{3n+1} \tag{31}$$

238 $$B_2 = 1 - \frac{(a+1)(1-S_i) - \left(a(a+2)b - (1-b)(1-S_i)\right)S_i^{3+2/n}}{\left(1-(1+ab)S_i\right)(a+2)} \tag{32}$$

239 The other parameter B_3, B_4 and B_5 can be calculated by Equation (15), Equation (22) and
240 Equation (23), respectively. Finally, Equation (16), Equation (19), Equation (21) and Equation
241 (24) constitute a special solution with the BC model compared to the general solution above. The
242 GAMS in the next part refers to this special solution.

3 Materials and methods

3.1 Model validation and evaluation

As an example, a loam soil with BC model parameters (θ_s = 0.434 cm cm^{-3}, θ_r = 0.027 cm cm^{-3}, n = 0.22, h_d = 11.15 cm, K_s = 0.022 cm min^{-1}) was used to validate the performance of the GAMS model. Additionally, the relations with the TGAM and GAME models were investigated regarding their different ways of treating the saturated zone. In order to avoid the disturbance of uncertain errors in real experiments on the theoretical evaluation, the numerical solution of HYDRUS-1D (Šimůnek et al., 2005) was used as the exact solution to produce the infiltration data needed to validate the new solution. The simulations were also conducted by both analytical and numerical methods to evaluate the influence of the developing saturated zone on infiltration.

The GAMS calculation was made following the procedures provided in section 2.2. The calculation of TGAM and GAME followed the same procedures descried in Ma et al. (2015). The numerical simulations of the Richards equation were conducted by the HYDRUS-1D software package (version 3.0) for the constant-head 1D vertical infiltration problem (Šimůnek et al., 2005). The soil column in the simulation was 200 cm in length with a discrete interval of 0.25 cm, and a uniform initial soil moisture distribution (θ_i = 0.04 cm cm^{-3}). The upper boundary of a constant water head (h_p = 0) and free drainage lower boundary were defined for the simulation. The infiltration time was 2800 min. The soil column was considered as semi-infinite, since the simulation was set to stop before the wetting front reaches the bottom. The simulated surface water flux, cumulative surface water flux, soil water flux and soil water content profiles at time steps of 10 min, 30 min, 60 min, 100 min, 500 min, 1000 min, 1500 min and 2000 min, were directly extracted from the simulated data by HYDRUS-1D. The lengths of the saturated zone (z_s) and wetted zone (z_f) were determined by checking the soil moisture profiles.

Specifically, on a soil moisture profile, the depth where soil water content began to be lower than θ_s was taken as z_s, and the depth where soil water content drop to θ_i was taken as z_f.

Relative error (RE) was employed to evaluate the deviation of the three models (GAMS, GAME and TGAM) from the numerical solution.

$$\mathrm{RE}_i = \frac{Y_i - O_i}{O_i} \times 100\% \tag{33}$$

where Y_i is the simulated value by analytical solutions (GAMS, GAME and TGAM); O_i is the observed value produced by HYDRUS-1D.

3.2 Estimation of model parameters

The new GAMS was numerically inverted to obtain the three parameters of soil hydraulic properties (n, h_d and K_s) from infiltration data (i.e. cumulative infiltration and wetted zone length versus time). Notably, the method based on the GAMS considered not only the unsaturated zone, which was ignored in the TGAM based methods (Ma et al., 2017), but also the developing saturated zone, which was neglected in the GAME method in the first stage of infiltration (Ma et al., 2017). The estimated soil hydraulic parameters by the methods based on GAMS, GAME and TGAM were compared to check the influence of the developing saturated zone on the estimation of soil hydraulic properties.

Furthermore, the time-dependent accuracy of analytical solution was investigated. The same loam soil (θ_s = 0.434 cm cm^{-3}, θ_r = 0.027 cm cm^{-3}, θ_i = 0.04 cm cm^{-3}, n = 0.22, h_d = 11.15 cm, K_s = 0.022 cm min^{-1}) was used as the tested soil. The observed time-lapse data (OBS) of cumulative infiltration and the length of wetted zone were produced by Hydrus-1D for the estimation of soil hydraulic parameters. Given the known parameters (θ_s = 0.434 cm cm^{-3}, θ_r = 0.027 cm cm^{-3}, θ_i =

287 0.04 cm cm^{-3}) and the unknown parameters (n, h_d and K_s), the Levenberg-Marquardt algorithm
288 was employed to minimize the objective function to estimate the unknown parameters (n, h_d and
289 K_s)

290 $$Q = \sum_{i=1}^{N} \left(\hat{I}_i \left(n, h_d, K_s \right) - I_i \right)^2 + \sum_{i=1}^{N} \left(\hat{z}_{f,i} \left(n, h_d, K_s \right) - z_{f,i} \right)^2 \quad (34)$$

291 where Q is the objective function; $\hat{I}_i$ and I_i are the simulated cumulative infiltration by the GAMS
292 and the observed data produced by HYDRUS-1D, respectively; $z_{f,i}$ and $\hat{z}_{f,i}$ are the length of
293 wetted zone simulated by the GAMS and the observed data produced by HYDRUS-1D,
294 respectively. Details of the methods based on the GAME and TGAM for estimating soil
295 hydraulic parameters from one-dimensional vertical infiltration can be found in Ma et al. (2017).

296 Moreover, the ratio of the saturated zone length to the effective wetted zone length (denoted
297 as $LR_{S/EW} = z_s/z_{fe}$ hereafter) in the GAMS was calculated based on Equation (18) and Equation
298 (21), and its sensitivities to soil texture (listed in Table 1), initial condition (θ_i) and boundary
299 condition (h_p) were investigated to theoretically analyze their influences on the development of
300 the saturated zone. The initial and boundary conditions were defined based on the loam soil (θ_s =
301 0.434 cm cm^{-3}, θ_r = 0.027 cm cm^{-3}, n = 0.22, h_d = 11.15 cm, K_s = 0.022 cm min^{-1}) with six values
302 of θ_i (i.e. 0.04 cm cm^{-3}, 0.08 cm cm^{-3}, 0.12 cm cm^{-3}, 0.16 cm cm^{-3}, 0.2 cm cm^{-3} and 0.25 cm cm^{-3}) for h_p = 0, and with six values of h_p (i.e. 0 cm, 2 cm, 5 cm, 10 cm, 15 cm and 20 cm) for θ_i =
304 0.04 cm cm^{-3}.

305

306 **Table 1.** Soil hydraulic properties of different textured soils (Hydrus-1D) and initial conditions
307 for numerical simulations.

Soil texture	θ_i cm cm^{-3}	θ_r cm cm^{-3}	θ_s cm cm^{-3}	n	h_d cm	K_s cm min^{-1}
Loamy Sand	0.05	0.035	0.401	0.474	8.70	0.1018
Sandy Loam	0.05	0.041	0.412	0.322	14.66	0.0432
Loam	0.04	0.027	0.434	0.220	11.15	0.0220
Silt	0.03	0.015	0.486	0.211	20.75	0.0113
Sandy Clay Loam	0.08	0.068	0.330	0.250	28.09	0.0072
Clay Loam	0.09	0.075	0.390	0.194	25.91	0.0038
Silty Clay Loam	0.08	0.040	0.432	0.151	32.57	0.0025
Sandy Clay	0.12	0.109	0.321	0.168	29.15	0.0020
Silty Clay	0.10	0.056	0.423	0.127	34.25	0.0015
Clay	0.12	0.090	0.385	0.131	37.31	0.0010

308

309 **4 Results**

310 4.1 The forward solution for infiltration simulation

311 As depicted in Figure 2 and Figure 3a, the surface water flux, cumulative surface water flux
312 and wetted zone length simulated by the GAMS with the parameters independently obtained
313 from soil hydraulic properties agree well with those simulated by HYDRUS-1D for the tested
314 loam soil. The relative errors of the simulated surface water flux, cumulative surface water flux
315 and wetted zone length are less than 8% for all time steps and less than 5% for most of the time
316 steps (Figure 4). The relative errors of these three infiltration variables are the highest at the
317 primary stage of the infiltration and gradually drops with the lapsed time. The simulated surface
318 water flux is very close to the exact solution with relative errors close to 0 after 500 min (Figure
319 4a). The relative errors of the simulated cumulative surface water flux and wetted zone length
320 decrease to about 2% after 500 min (Figure 4b and 4c). As shown in Figure 3b, the GAMS give
321 accurate estimates of the saturated zone length all along the time. However, the GAMS seems to

322 slightly overestimate the length of the unsaturated zone but with no increasing deviation (Figure
323 3c). This should be responsible for the 2% relative errors of the simulated cumulative surface
324 water flux and wetted zone length in the later stage of the infiltration. Generally, the soil
325 moisture profiles simulated by the GAMS agree well with the those simulated by HYDRUS-1D
326 from a long time perspective but slight deviation exists in the initial short time of infiltration
327 (Figure 5).

328 In general, the novel GAMS model enables a more accurate simulation of infiltration
329 process than the GAME and TGAM models for a loam soil (Figures 2-5). Obviously, the TGAM
330 overestimated the surface water flux, cumulative surface water flux, and the length of the wetted
331 zone with REs of about 10%-18%. The GAME underestimated the surface water flux,
332 cumulative surface water flux and the length of wetted zone with REs of about 10%. The GAMS
333 gave the best simulations with the smallest and decreasing REs among the three models. Only in
334 the first stage of infiltration, the simulation accuracy of the GAME (Figure 4) is comparable to
335 and even higher than the GAMS (Figure 4c, Figure 5). However, in the first stage of infiltration,
336 the GAME shows increasing errors (Figure 3c, Figure 4). In the second stage of infiltration, the
337 surface water flux was still underestimated by the GAME with REs of about -10%. It should be
338 noted that the GAME simulated the soil moisture profiles better than the GAMS in the first stage
339 but the REs of the GAME substantially increased after the critical time (Figure 5).

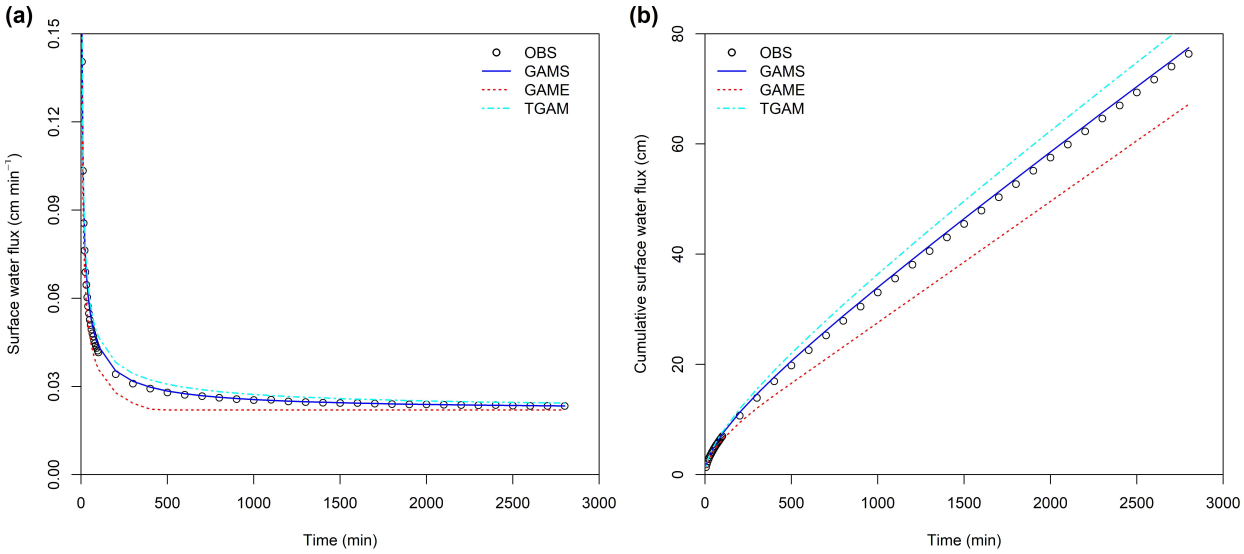

340

341 **Figure 2**. Simulated (a) surface water flux, and (b) cumulative surface water flux by the GAMS,

342 GAME and TGAM, respectively, compared with the observed data (OBS) produced by the

343 numerical solution (HYDRUS-1D) for a loam soil.

344

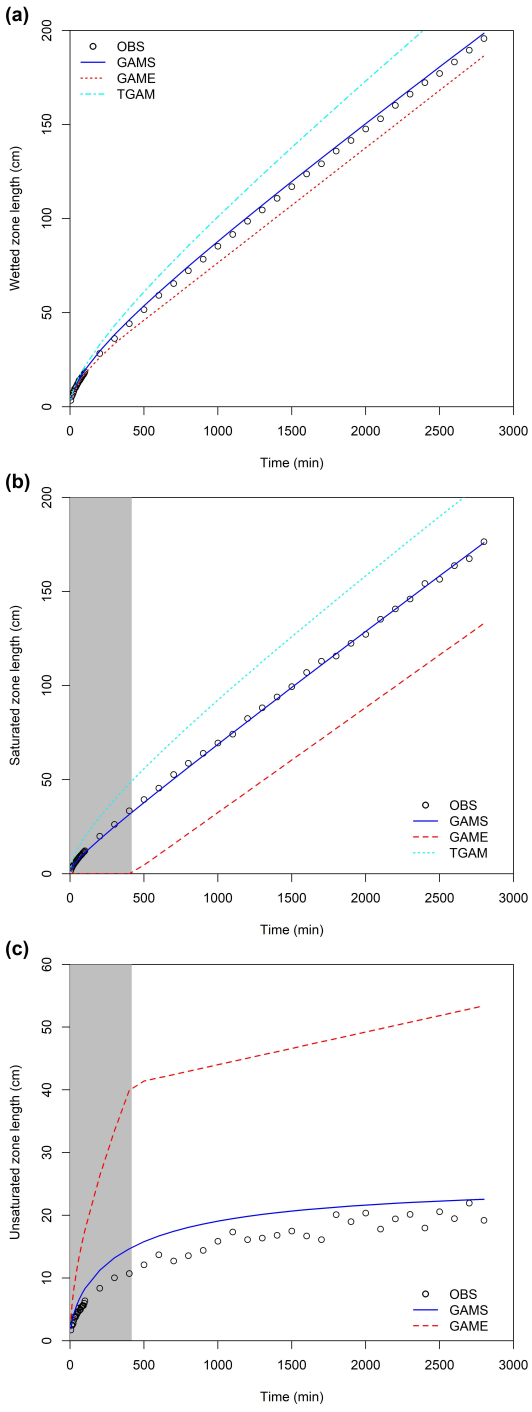

345

346 **Figure 3**. Simulated lengths of (a) wetted zone, (b) saturated zone, and (c) unsaturated zone by
347 the GAMS, GAME and TGAM, respectively, compared with the observed data (OBS) produced
348 by the numerical solution (HYDRUS-1D) for a loam soil.

349

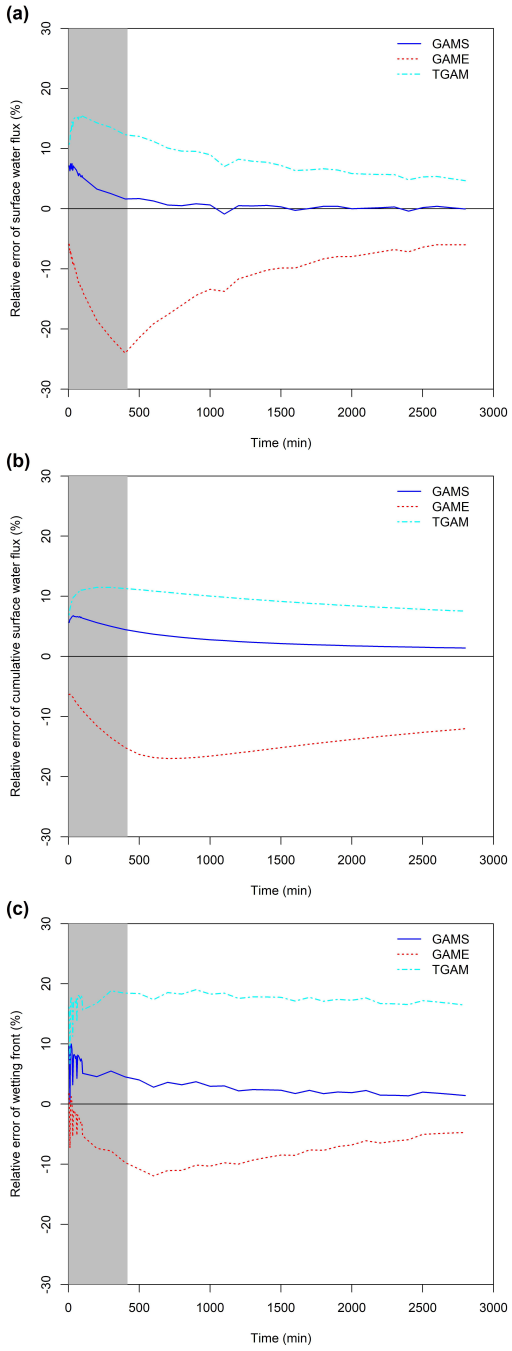

Figure 4. Relative error (RE) of (a) surface water flux, (b) cumulative surface water flux and (c) length of wetted zone simulated by the GAMS, GAME and TGAM, respectively, to that by the numerical solution (HYDRUS-1D) for a loam soil. The gray zone represents the infiltration before the critical time calculated by equation (29) in Ma et al. (2015).

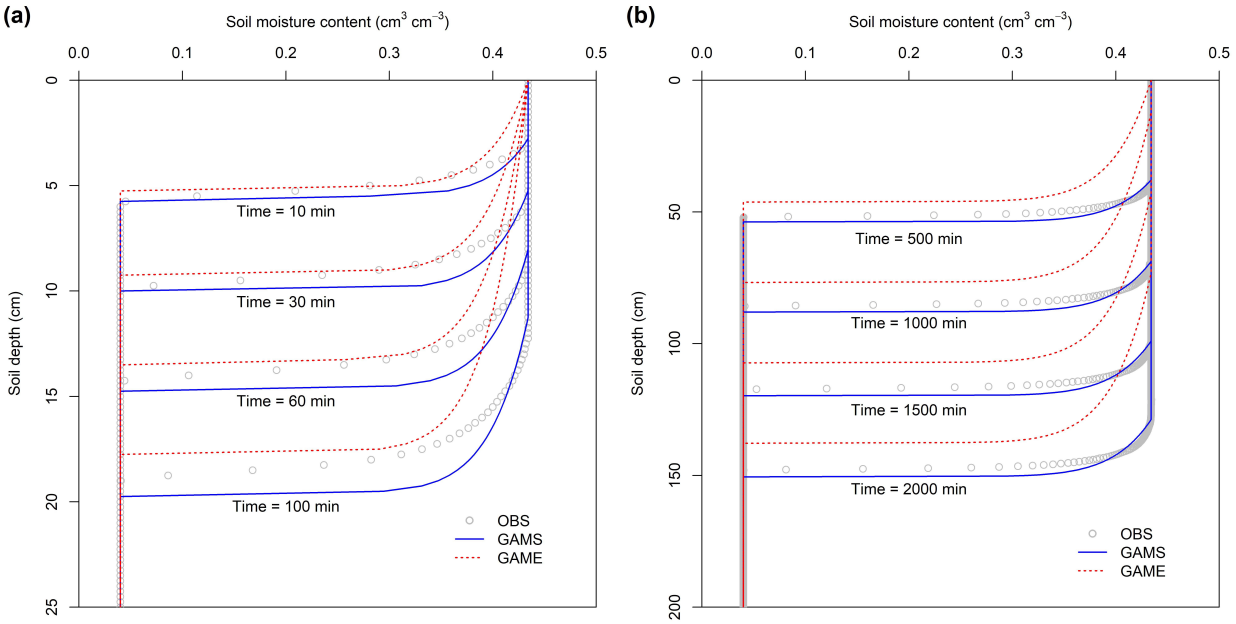

Figure 5. Simulated soil moisture profiles in (a) short infiltration time and (b) long infiltration time by the GAMS and GAME, respectively, compared with the observed data (OBS) produced by the numerical solution (HYDRUS-1D) for a loam soil.

4.2 The influence of saturated zone on the estimation of soil hydraulic properties

Figure 6 shows the estimated parameters of soil hydraulic properties for a loam soil by inverting the GAMS, GAME and TGAM models. The estimated values of n and h_d by these three models exhibit a similar decline tendency along the infiltration time, while the estimated values of K_s increase with the infiltration time. Generally, the estimated parameters by the GAMS are closer to the real values compared with those by the GAME. The values of n estimated by the TGAM is equal to those by the GAME, while the estimated values of h_d and K_s by the TGAM are close to those by the GAMS. The results indicate that the critical time is important for the estimation accuracy of the hydraulic parameters. Before the critical time, especially in a short time, the estimated parameters by the GAME show relatively lower errors than that by the GAMS. After the critical time, however, the estimation by the GAMS exhibits a

higher accuracy than that by the GAME. Whether in a short or long time, the inverting of the TGAM cannot simultaneously give accurate estimates of n, h_d and K_s. Generally, the GAMS improved the estimate accuracy of soil hydraulic properties by the infiltration models from the infiltration process after the critical time.

4.3 The sensitivity analysis of saturated zone length

As shown in Figure 7, $LR_{S/EW}$ can be affected by soil properties (i.e. soil texture), boundary conditions (i.e. surface water depth), and initial conditions (i.e. initial soil water content). Without ponding water over soil surface, the values of $LR_{S/EW}$ were initially equal to 0.5, increased with infiltration time and approached to 1 at infinity. Increased ponding depth can promote the proportion of the saturated zone especially at the initial stage of infiltration but its effects attenuate with time (Figure 7a). The $LR_{S/EW}$ increased with elevating initial soil water content while little influence can be found at the initial stage of infiltration (Figure 7b). Obviously, soil texture shows the greatest effect on the development of saturated zone (Figure 7c). The $LR_{S/EW}$ for a clay soil increased slowly with time and was close to 0.5 for most of time. The results indicate that the coarser the soil texture, the greater the $LR_{S/EW}$ at the same infiltration time. The $LR_{S/EW}$ for a loamy sandy soil increased rapidly and approached to 1 as infiltration continued.

As shown in Figure 8a, $LR_{S/EW}$ can also be affected by soil hydraulic properties, that is, the shape coefficient n of soil water retention curve, water-entry suction h_d, and saturated hydraulic conductivity K_s. A higher n value caused a lower fraction of saturated zone (Figure 8a) during infiltration. A greater value of h_d resulted in a lower $LR_{S/EW}$ (Figure 8b). A higher value of K_s accelerated the development of z_s (Figure 8c). Compared to h_d and K_s, the influence of the shape coefficient n on $LR_{S/EW}$ seems to be negligible.

394

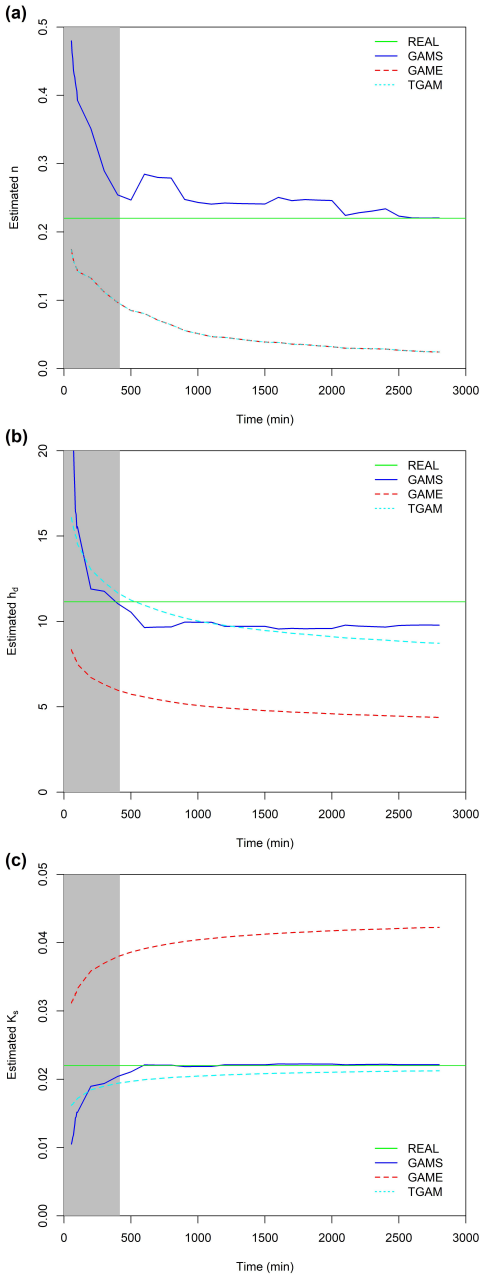
(a)
Estimated n
Time (min)
REAL
GAMS
GAME
TGAM
(b)
Estimated h_d
Time (min)
REAL
GAMS
GAME
TGAM
(c)
Estimated K_s
Time (min)
REAL
GAMS
GAME
TGAM

395

396 **Figure 6**. Time-dependent (a) shape coefficient n, (b) water-entry suction h_d, and (c) saturated
397 hydraulic conductivity K_s estimated by model inversion of GAMS, GAME and TGAM,
398 respectively, with the observed data of different infiltration time, compared with the real
399 parameter values (REAL) of a loam soil. The gray zone represents the infiltration before the
400 critical time calculated by equation (29) in Ma et al. (2015).

401

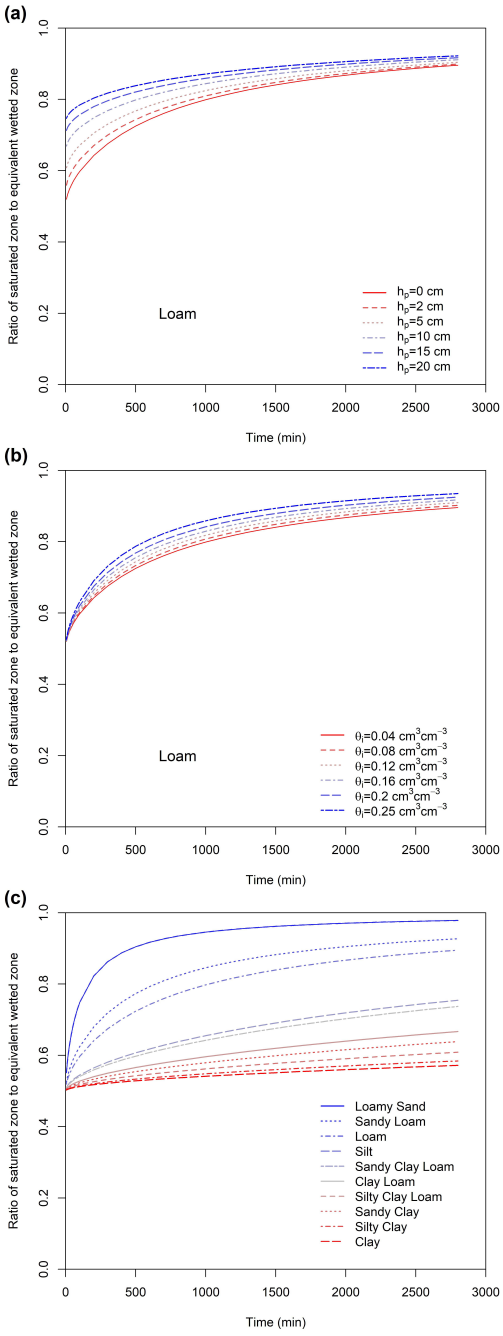
(a)
Ratio of saturated zone to equivalent wetted zone
Loam
h_p=0 cm
h_p=2 cm
h_p=5 cm
h_p=10 cm
h_p=15 cm
h_p=20 cm
Time (min)
(b)
Ratio of saturated zone to equivalent wetted zone
Loam
θ_i=0.04 cm^3cm^{-3}
θ_i=0.08 cm^3cm^{-3}
θ_i=0.12 cm^3cm^{-3}
θ_i=0.16 cm^3cm^{-3}
θ_i=0.2 cm^3cm^{-3}
θ_i=0.25 cm^3cm^{-3}
Time (min)
(c)
Ratio of saturated zone to equivalent wetted zone
Loamy Sand
Sandy Loam
Loam
Silt
Sandy Clay Loam
Clay Loam
Silty Clay Loam
Sandy Clay
Silty Clay
Clay
Time (min)

402

403 **Figure 7**. Sensitive analysis of the length ratio of saturated zone to equivalent wetted zone
404 $LR_{S/EW}$ to (a) surface water depth (h_p= 0 cm, 2 cm, 5 cm, 10 cm, 15 cm and 20 cm) for a loam
405 soil, (b) initial soil water content (θ_i = 0.04 cm cm^{-3}, 0.08 cm cm^{-3}, 0.12 cm cm^{-3}, 0.16 cm cm^{-3},
406 0.2 cm cm^{-3} and 0.25 cm cm^{-3}) for a loam soil, and (c) soil texture (see in Table 1) by using the
407 GAMS.

408

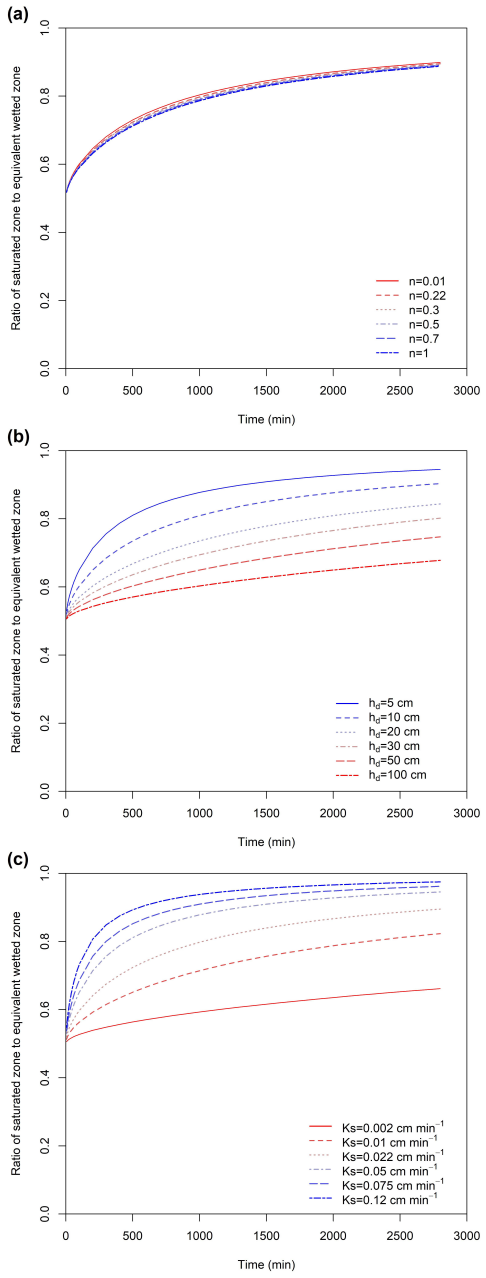

409

Figure 8. Sensitive analysis of the length ratio of saturated zone to equivalent wetted zone $LR_{S/EW}$ to (a) the shape coefficient n (n = 0.01, 0.22, 0.3, 0.5, 0.7 and 1), (b) water-entry suction h_d (h_d = 5 cm, 10 cm, 20 cm, 30 cm, 50 cm and 100 cm), and (c) saturated hydraulic conductivity K_s (K_s = 0.002 cm min^{-1}, 0.01 cm min^{-1}, 0.022 cm min^{-1}, 0.05 cm min^{-1}, 0.075 cm min^{-1} and 0.12 cm min^{-1}) for a loam soil by using the GAMS.

5 Discussion

5.1 The factors influencing the development of saturated zone

The results in Figure 7a agree well with the early research by Philip (1958b). A higher ponding depth on the surface can promote the development of saturated zone, which can be deduced by Equation (12) and Equation (15). Initially wetter soils have smaller space for further water storage and narrower range of soil moisture in the wetted zone. Thus, the saturated zone developed more quickly in a wet soil than in a dry soil (Philip, 1958a), which was confirmed by the results in Figure 7b.

Soil texture could affect the development of saturated zone mainly from three aspects: (a) the shape coefficient n, which reflects soil pore size distribution; (b) water-entry suction h_d, which is related to the maximum equivalent capillary pore size of a soil, and (c) saturated hydraulic conductivity K_s. A higher n value represents a steeper pore size distribution which is closer to the delta-type soil water diffusivity and could cause a lower fraction of saturated zone during infiltration as shown in Figure 8a. Since soil is tension-saturated when $0 > h > -h_d$ (Philip, 1958a), the water-entry suction shall have contrary impacts on the saturated zone to h_p from Equation (12) and Equation (15). A greater value of h_d resulted in a lower $LR_{S/EW}$. The parameter

B_4 is the average velocity of pore water under gravity gradient which corresponds to the cases in a large infiltration time. For a given soil porosity, B_4 is positively correlated to K_s. According to Equation (21), a higher value of K_s will accelerate the development of z_s as shown in Figure 8c. In contrast to a fine-textured soil, a coarse-textured soil normally has greater K_s and n but lower h_d. Obviously, the positive effects of K_s and h_d on $LR_{S/EW}$ overwhelmed the negative effect of n, which can explain the results shown in Figure 7c.

5.2 The influence of saturated zone on infiltration

The key character differentiating the GAMS from the TGAM and GAME models is its consideration of the wetting zone composed of both saturated and unsaturated zones. The TGAM was derived by assuming a piston-type soil moisture profile, that is, a fully saturated wetting zone (Green & Ampt, 1911). While, in the GAME, the wetting zone was considered unsaturated before a critical time, when the surface water flux dropped to K_s, and after which the saturated zone developed linearly with time (Ma et al., 2015). Insight into the internal relationships of the GAMS with the TGAM and GAME could provide an improved understanding on the influence of the saturated zone on infiltration.

With the definition of Equation (18), the Equation (12) can be rewritten as

$$J_{w0} = K_s\left(1+\frac{B_1+B_3}{z_{fe}}\right)-K_sB_2\left(1-\frac{z_s}{z_{fe}}\right) \tag{35}$$

The first term on the right side of Equation (35) is equal to the TGAM which is characterized by piston-type water profile and average pressure head at the wetting front (i.e. Equation (13)) with the form of Neuman (1976). The second term on the right side of Equation (35) represents the influence of the saturated zone on surface soil water flux. For a soil with delta-type water

453 diffusivity, a piston-type water profile is expected and z_s is close to z_{fe}. Then, the GAMS
454 (Equation (35)) can be transformed to the TGAM, given:

455 $$J_{w0} = K_s\left(1+\frac{B_1+B_3}{z_{fe}}\right) \quad (36)$$

456 For a soil with water diffusivity far from delta-type, a non-piston-type water profile and a
457 low length ratio of the saturated zone to wetted zone are expected. If neglecting the development
458 of saturated zone (i.e. $z_s = 0$), the GAMS (Equation (35)) can be transformed to the GAME, that
459 is,

460 $$J_{w0} = K_s\left(1+\frac{B_1+B_3}{z_{fe}}\right) - K_s B_2 = (1-B_2)K_s\left(1+\frac{B_1+B_3}{(1-B_2)z_{fe}}\right) \quad (37)$$

461

462 As depicted in Equation (35), it is $LR_{S/EW}$ rather than the saturated zone length that leads the
463 transformations of the GAMS model to GAME and TGAM models. Obviously, the TGAM
464 overestimated the surface water flux and thus cumulative surface water flux, and the length of
465 the wetted zone because the wetting zone was considered overall saturated as shown in Equation
466 (36). Neglecting the development of the saturated zone as shown in Equation (37) resulted in the
467 underestimation of the surface water flux by the GAME. In contrast, a developing saturated zone
468 was accurately characterized in the GAMS as shown in Equation (35), which contributed to the
469 best simulations among the three models.

470 However, in the first stage of infiltration, $LR_{S/EW}$ was relatively small (Figure 7) and same
471 to the effects of saturated zone on the surface water flux. In addition, the soil moisture profile
472 shape in GAME was closer to the real one in the first stage than that in the GAMS (Figure 9),

473 which will be discussed in details in the section 5.3. Consequently, the simulation or estimation
474 accuracy of the GAME (Figure 4) is comparable to and even higher than the GAMS (Figure 4c,
475 Figure 5) in the first stage of infiltration. Nevertheless, $LR_{S/EW}$ and the effects of saturated zone
476 on the surface water flux increased with time (Figure 7). Then, the simulation errors of the
477 GAME rose up (Figure 3c, Figure 4) as the saturated zone was completely ignored (Figure 3b).
478 Although a linearly increasing saturated zone length was considered in the second stage of
479 infiltration (Figure 3b), it is not enough to fully characterize the developing saturated zone and
480 thus the surface water flux was still underestimated.

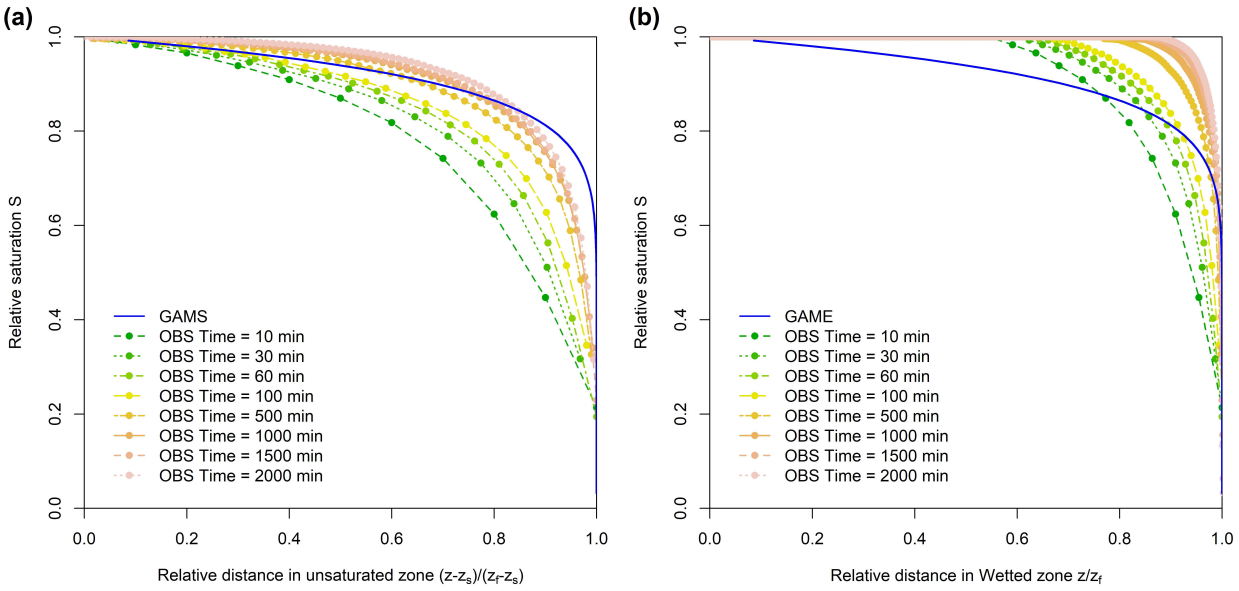

481

482 **Figure 9**. Comparison of the simulated relative soil moisture profile by (a) the GAMS, and (b)
483 the GAME to the observed data (OBS) produced by the numerical solution (HYDRUS-1D) for a
484 loam soil.

485 5.3 The factors causing the deviation of the GAMS

486 That the GAMS exhibits relatively larger errors in the simulated water fluxes in short
487 infiltration times than those in long infiltration times could be induced by the two assumptions of

488 time-independency in soil water flux-saturation relationship (Equation (7)) and relative soil
489 moisture profile (Equation (3)) in the unsaturated zone for the derivation of the GAMS.

490 According to the theoretical analysis by Philip (1973), the soil water flux-saturation
491 relationship in the form of Equation (7) represents the case of coarse-textured soils, that are,
492 linear soils or "delta-function" soils. For natural soils, it may vary with soil texture, infiltration
493 time and boundary conditions but will converge to the curve of Equation (7) in the long
494 infiltration time (Philip, 1973). The texture-dependency of soil water flux-saturation relationship
495 has been confirmed by the observed data in White (1979) and Ma et al. (2017). More accurate
496 expressions for the soil water flux-saturation relationship can be found in literatures (Evangelides
497 et al., 2005; Kargas et al., 2019; Ma et al., 2017; Vauclin and Haverkamp, 1985). Actually, the
498 soil water flux-saturation relationship depended little on time especially in a short infiltration
499 period (Ma et al., 2017) and did not exert obvious influences on infiltration simulations
500 (Haverkamp et al., 1990; Hogarth et al., 2011). Moreover, the expression of Equation (7) has
501 been successfully used for deriving accurate approximate analytical solutions of infiltration
502 problems from Richards equation (Assouline, 2013; Haverkamp et al., 1990; Hogarth et al.,
503 2011; Ma et al., 2015). Although more accurate expression than Equation (7) can be adapted to
504 improve the infiltration simulation (Hayek, 2018), the corresponded solutions are more complex
505 for practical application. For the loam soil in this research, no obvious time-dependency can be
506 found in the soil water flux-saturation relationship and the Equation (7) in the GAMS exhibits
507 enough accuracy as shown in Figure 10. It seems impossible that the relatively great errors of the
508 surface water flux simulated by the GAMS (Figure 4) was caused by the assumption of soil
509 water flux-saturation relationship inherent in Equation (7).

510 The assumption of time-dependent soil moisture profile shape simplified the derivation of
511 the GAMS. Actually, the relative soil moisture profile in the unsaturated zone for the loam soil
512 exhibits time-dependency in short infiltration time and approaches to a steady shape only in long
513 infiltration time (Figure 9). Consequently, the deviation of the simulated soil moisture profiles by
514 the GAMS from those by HYDRUS-1D is mainly in the early infiltration stage and exhibits in
515 two aspects (Figure 5): (1) the overestimated length of unsaturated zone, (2) the twisted shape of
516 soil moisture profiles in the unsaturated zone. Including the developing saturated zone makes the
517 simulated relative soil moisture profiles by the GAMS closer to the steady shape in the long
518 infiltration time (Figure 9a) while the GAME yielded a relative soil moisture profile closer to the
519 unsteady shape in the short time for no consideration of saturated zone (Figure 9b). In addition,
520 the expression for calculating the length of unsaturated zone was derived based on the soil
521 moisture profile of Equation (3) in the unsaturated zone. Therefore, it could be concluded that
522 the simulation errors of the GAMS in the short time is mainly induced by the errors in the
523 function of relative soil moisture profile in the unsaturated zone.

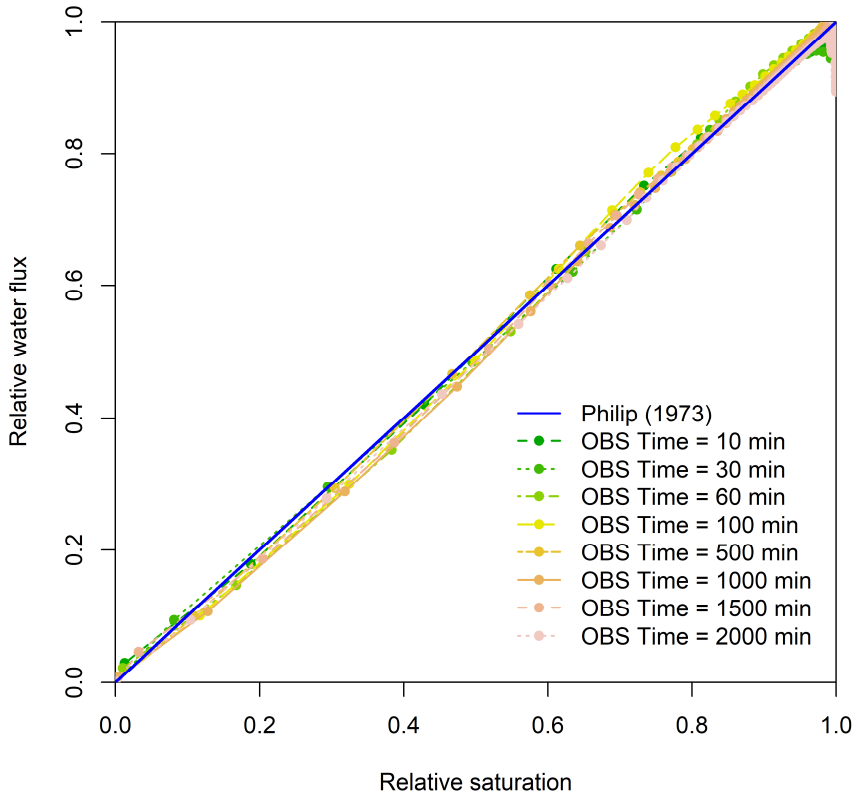

524

525 **Figure 10**. Comparison of the simulated soil water flux-saturation relationship by the numerical
526 solution (HYDRUS-1D) and the expression proposed by Philip (1973) for a loam soil.

527

528 Actually, the expression of the relative soil moisture profile (i.e. Equation (3)) in both the
529 GAME and GAMS was derived based on Equation (7) and an approximation of time-
530 independent soil potential profile shape (Equation (A6) in Ma *et al.* (2015). A more accurate
531 description of soil water flux-saturation relationship and the consideration of the time-
532 dependency of soil moisture profile shape are expected to further improve the accuracy of soil
533 moisture profile simulation (Hayek, 2018; Hogarth et al., 2013; Hogarth et al., 2011).
534 Unfortunately, it is difficult to derive such a time-dependent expression of soil moisture profile
535 shape in the current study, given the complex relationship between soil moisture profile and soil

536 water flux (Haverkamp et al., 1990; Hogarth et al., 2011). A recent work by Su et al. (2018)
537 proposed an expression of time-dependent soil moisture profile shape. However, it makes the
538 derivation of infiltration model difficult and fails at a large infiltration time.

539 5.4 The general use of the GAMS

540 Based on the assumptions of time-independency of soil water flux-saturation relationship
541 and relative soil moisture profile, the GAMS was derived with no limitation of the specific form
542 of relative soil moisture profile and soil hydraulic properties. According to Wang et al. (2013)
543 and Ma et al. (2015, 2017b), the form of relative soil moisture profile depends on the specific
544 function of soil hydraulic properties and soil water flux-saturation relationship, and the shape
545 coefficient of soil moisture profile is only related with the shape parameter of the soil water
546 retention curve. Given the soil moisture profile function derived for a specific soil hydraulic
547 property model (e.g. BC model, VG model), it is easy to obtain the parameters of the GAMS by
548 Equation (9), Equations (13)-(15) and Equations (22)-(23) from soil hydraulic properties.
549 Furthermore, other forms of soil water flux-saturation relationship (Evangelides et al., 2005; Ma
550 et al., 2017) can be also included in the novel GAMS by substituting the soil water flux-
551 saturation relationship in Philip (1973).

552 In the future, more accurate unsaturated soil moisture profile functions are expected to be
553 adopted in the GAMS to further improve the infiltration simulation and soil hydraulic parameters
554 estimation. Moreover, the general solution of the GAMS should be extended from uniform soils
555 to stratified soils or soils with non-uniform initial soil moisture profile, as well as the soils with
556 more hydraulic property models such as the VG model (van Genuchten, 1980).

6 Conclusions

Ponding at the soil surface changes surface pressure head and affects soil moisture profile shape in infiltration. A novel analytical solution, the GAMS, is derived to one-dimensional vertical infiltration under ponding conditions for any forms of soil hydraulic properties models, which can describe the length of saturated zone versus infiltration time with a simple expression. The GAMS was evaluated with a special solution for Brooks-Corey soil hydraulic property model. Compared with the TGAM model (Green and Ampt, 1911) and GAME model (Ma et al., 2015), the GAMS showed a better performance in infiltration simulation indicated by higher agreement with the numerical solution by HYDRUS-1D along the infiltration period. Furthermore, the model inversion of the GAMS yields more accurate estimates of soil hydraulic property model parameters from a one-dimensional vertical infiltration experiment. Besides, the time-dependency of model parameter estimation by the GAMS is weaker in long infiltration time than the TGAM and GAME models. The novel GAMS is supposed to be used in irrigation design and rainfall-runoff simulation by providing more accurate data of cumulative infiltration and soil moisture distribution.

Acknowledgments

This work was supported by the National Natural Science Foundation of China (No. 42177292), the Strategic Priority Research Program of the Chinese Academy of Sciences (Grant No. XDA28010401), and the earmarked fund for China Agriculture Research System (CARS-03, CARS-52).

Data Availability Statement

The data set used to validate the new solution was produced by the HYDRUS-1D software (version 3.0) (Šimůnek et al., 2005). The program to calculate and draw figures is edited in R language (version 4.1.2) (R Core Team, 2021). All the data set and program are available after requested.

References

Angulo-Jaramillo, R., V. Bagarello, S. Di Prima, A. Gosset, M. Iovino, and L. Lassabatere (2019), Beerkan Estimation of Soil Transfer parameters (BEST) across soils and scales, *Journal of Hydrology*, *576*, 239-261. doi:10.1016/j.jhydrol.2019.06.007

Assouline, S. (2013), Infiltration into soils: Conceptual approaches and solutions, *Water Resources Research*, *49*(4), 1755-1772. doi:10.1002/wrcr.20155

Assouline, S., J. S. Selker, and J. Y. Parlange (2007), A simple accurate method to predict time of ponding under variable intensity rainfall, *Water Resources Research*, *43*(3), W03426. doi:10.1029/2006wr005138

Bonetti, S., Z. W. Wei, and D. Or (2021), A framework for quantifying hydrologic effects of soil structure across scales, *Commun Earth Environ*, *2*(1). doi:10.1038/s43247-021-00180-0

Brutsaert, W. (1977), Vertical infiltration in dry soil, *Water Resources Research*, *13*(2), 363-368. doi:10.1029/WR013i002p00363

598 Burdine, N. T. (1953), Relative Permeability Calculations from Pore Size Distribution Data, *T*
599 *Am I Min Met Eng*, *198*, 71-78. doi:10.2118/225-G
600 Corradini, C., F. Melone, and R. E. Smith (1994), Modeling Infiltration during Complex Rainfall
601 Sequences, *Water Resources Research*, *30*(10), 2777-2784. doi:10.1029/94wr00951
602 Corradini, C., F. Melone, and R. E. Smith (1997), A unified model for infiltration and
603 redistribution during complex rainfall patterns, *Journal of Hydrology*, *192*(1-4), 104-124.
604 doi:10.1016/S0022-1694(96)03110-1
605 Evangelides, C., C. Tzimopoulos, and G. Arampatzi (2005), Flux-saturation relationship for
606 unsaturated horizontal flow, *Soil Science*, *170*(9), 671-679.
607 doi:10.1097/01.ss.0000185904.72717.4c
608 Fatichi, S., D. Or, R. Walko, H. Vereecken, M. H. Young, T. A. Ghezzehei, T. Hengl, S. Kollet,
609 N. Agam, and R. Avissar (2020), Soil structure is an important omission in Earth System
610 Models, *Nat Commun*, *11*(1), 522. doi:10.1038/s41467-020-14411-z
611 Green, W. H., and G. A. Ampt (1911), Studies on Soil Phyics, *The Journal of Agricultural*
612 *Science*, *4*(01), 1-24. doi:10.1017/S0021859600001441
613 Haverkamp, R., P. J. Ross, K. R. J. Smettem, and J. Y. Parlange (1994), 3-dimensional analysis
614 of infiltration from the disc infiltrometer .2. physically-based infiltration equation, *Water*
615 *Resources Research*, *30*(11), 2931-2935. doi:10.1029/94wr01788
616 Haverkamp, R., J. Y. Parlange, J. L. Starr, G. Schmitz, and C. Fuentes (1990), Infiltration under
617 Ponded Conditions .3. A Predictive Equation Based on Physical Parameters, *Soil Science*,
618 *149*(5), 292-300. doi:10.1097/00010694-199005000-00006
619 Hayek, M. (2018), An efficient analytical model for horizontal infiltration in soils, *Journal of*
620 *Hydrology*, *564*, 1120-1132. doi:10.1016/j.jhydrol.2018.07.058

621 Hogarth, W. L., D. A. Lockington, D. A. Barry, M. B. Parlange, R. Haverkamp, and J. Y.
622 Parlange (2013), Infiltration in soils with a saturated surface, *Water Resources Research*,
623 *49*(5), 2683-2688. doi:10.1002/wrcr.20227
624 Hogarth, W. L., D. A. Lockington, D. A. Barry, M. B. Parlange, G. C. Sander, L. Li, R.
625 Haverkamp, W. Brutsaert, and J. Y. Parlange (2011), Analysis of time compression
626 approximations, *Water Resources Research*, *47*, W09501. doi:10.1029/2010WR010298
627 Horton, R. E. (1941), An Approach Toward a Physical Interpretation of Infiltration-Capacity, *Soil*
628 *Science Society of America Journal*, *5*(C), 399-417.
629 doi:10.2136/sssaj1941.036159950005000C0075x
630 Jaiswal, P., Y. Gao, M. Rahmati, J. Vanderborght, J. Šimůnek, H. Vereecken, and J. A. Vrugt
631 (2022), Parasite inversion for determining the coefficients and time-validity of Philip's two-
632 term infiltration equation, *Vadose Zone J.*, *21*(1), e20166. doi:10.1002/vzj2.20166
633 Kargas, G., and P. A. Londra (2021), Comparison of Two-Parameter Vertical Ponded Infiltration
634 Equations, *Environmental Modeling & Assessment*, *26*(2), 179-186. doi:10.1007/s10666-
635 020-09727-5
636 Kargas, G., P. Londra, and P. Kerkides (2019), Investigation of the Flux–Concentration Relation
637 for Horizontal Flow in Soils, *Water*, *11*(12), 2442. doi:10.3390/w11122442
638 Klopp, H. W., and A. L. M. Daigh (2020), Soil hydraulic model parameters and methodology as
639 affected by sodium salt solutions, *Soil Sci Soc Am J*, *84*(2), 354-370. doi:10.1002/saj2.20015
640 Kostiakov, A. N. (1932), On the Dynamics of the Coefficient of Water Percolation in Soils and
641 on the Necessity for Studying it from a Dynamic Point of View for Purpose of Amelioration,
642 paper presented at Transactions of 6th Committee International Society of Soil Science,
643 Russia.

644 Ma, D. H., Q. J. Wang, and M. A. Shao (2009), Analytical Method for Estimating Soil Hydraulic
645 Parameters from Horizontal Absorption, *Soil Science Society of America Journal*, *73*(3),
646 727-736. doi:10.2136/sssaj2008.0050
647 Ma, D. H., J. B. Zhang, and Y. X. Lu (2017), Derivation and Validation of a New Soil Pore-
648 Structure-Dependent Flux–Saturation Relationship, *Vadose Zone J.*, *16*(5).
649 doi:10.2136/vzj2016.11.0117
650 Ma, D. H., J. B. Zhang, J. B. Lai, and Q. J. Wang (2016), An improved method for determining
651 Brooks–Corey model parameters from horizontal absorption, *Geoderma*, *263*, 122-131.
652 doi:10.1016/j.geoderma.2015.09.007
653 Ma, D. H., J. B. Zhang, Y. X. Lu, L. s. Wu, and Q. J. Wang (2015), Derivation of the
654 Relationships between Green–Ampt Model Parameters and Soil Hydraulic Properties, *Soil*
655 *Science Society of America Journal*, *79*(4), 1030-1042. doi:10.2136/sssaj2014.12.0501
656 Ma, D. H., J. B. Zhang, R. Horton, Q. J. Wang, and J. B. Lai (2017), Analytical Method to
657 Determine Soil Hydraulic Properties from Vertical Infiltration Experiments, *Soil Science*
658 *Society of America Journal*, *81*(6), 1303-1314. doi:10.2136/sssaj2017.02.0061
659 Mezencev, V. J. (1948), Theory of formation of the surface runoff, *Meteorol I Gidrologia*(3), 33–
660 46
661 Morbidelli, R., C. Corradini, C. Saltalippi, A. Flammini, J. Dari, and R. S. Govindaraju (2018),
662 Rainfall Infiltration Modeling: A Review, *Water*, *10*(12). doi:10.3390/w10121873
663 Moret-Fernández, D., B. Latorre, M. V. López, Y. Pueyo, L. Lassabatere, R. Angulo-Jaramilo, M.
664 Rahmati, J. Tormo, and J. M. Nicolau (2020), Three- and four-term approximate expansions
665 of the Haverkamp formulation to estimate soil hydraulic properties from disc infiltrometer
666 measurements, *Hydrological Processes*, *34*(26), 5543-5556. doi:10.1002/hyp.13966

667 Neuman, S. P. (1976), Wetting Front Pressure Head in Infiltration-Model of Green and Ampt,
668 *Water Resources Research*, *12*(3), 564-566. doi:10.1029/WR012i003p00564
669 Parlange, J. Y. (1971), Theory of Water-Movement in Soils .2. One-Dimensional Infiltration, *Soil*
670 *Science*, *111*(3), 170-174
671 Parlange, J. Y. (1972), Theory of Water Movement in Soils .6. Effect of Water Depth over Soil,
672 *Soil Science*, *113*(5), 308-312
673 Parlange, J. Y. (1975), Note on Green and Ampt Equation, *Soil Science*, *119*(6), 466-467
674 Parlange, J. Y., I. Lisle, and R. D. Braddock (1982), The Three-Parameter Infiltration Equation,
675 *Soil Science*, *133*(6), 337-341
676 Philip, J. R. (1957a), The Theory of Infiltration: 1. the Infiltration Equation and Its Solution, *Soil*
677 *Science*, *83*(5), 345-358
678 Philip, J. R. (1957b), The Theory of Infiltration: 4. Sorptivity and Algebraic Infiltration
679 Equations, *Soil Science*, *84*(3), 257-264
680 Philip, J. R. (1958a), The Theory of Infiltration: 7, *Soil Science*, *85*(6), 333-337
681 Philip, J. R. (1958b), The Theory of Infiltration: 6 Effect of Water Depth Over Soil, *Soil Science*,
682 *85*(5), 278-286
683 Philip, J. R. (1969), Theory of Infiltration, *Adv. Hydrosci*, *5*, 215-296
684 Philip, J. R. (1973), On solving the unsaturated flow equation: 1. The flux-concentration relation,
685 *Soil Science*, *116*(5), 328-335
686 Rahmati, M., M. Rezaei, L. Lassabatere, R. Morbidelli, and H. Vereecken (2021), Simplified
687 characteristic time method for accurate estimation of the soil hydraulic parameters from one-
688 dimensional infiltration experiments, *Vadose Zone J.*, *20*. doi:10.1002/vzj2.20117
689 Richards, L. A. (1931), Capillary conduction of liquids through porous mediums, *Physics*, *1*,

690 318-333. doi:10.1063/1.1745010
691 R Core Team (2021). R: A language and environment for statistical computing. R Foundation for
692 Statistical Computing, Vienna, Austria. URL https://www.R-project.org/.
693 Selker, J. S., and S. Assouline (2017), An explicit, parsimonious, and accurate estimate for
694 ponded infiltration into soils using the Green and Ampt approach, *Water Resources*
695 *Research*, *53*(8), 7481-7487. doi:10.1002/2017wr021020
696 Šimůnek, J., M. T. van Genuchten, and M. Šejna (2005), The HYDRUS-1D Software Package
697 for Simulating the Movement of Water, Heat, and Multiple Solutes in Variably Saturated
698 Media, in *HYDRUS Software Series 1*, edited, Department of Environmental
699 Sciences,University of California Riverside, Riverside, California, USA.
700 Stewart, R. D. (2019), A Generalized Analytical Solution for Preferential Infiltration and
701 Wetting, *Vadose Zone J.*, *18*(1), 180148. doi:10.2136/vzj2018.08.0148
702 Stewart, R. D., D. E. Rupp, M. R. Abou Najm, and J. S. Selker (2013), Modeling effect of initial
703 soil moisture on sorptivity and infiltration, *Water Resources Research*, *49*(10), 7037-7047.
704 doi:10.1002/Wrcr.20508
705 Su, L., X. Yang, Q. Wang, X. Qin, B. Zhou, and Y. Shan (2018), Functional Extremum Solution
706 and Parameter Estimation for One-Dimensional Vertical Infiltration using the Brooks–Corey
707 Model, *Soil Science Society of America Journal*, *82*(6), 1319-1332.
708 doi:10.2136/sssaj2018.01.0016
709 Swartzendruber, D. (1987), A quasi-solution of richards equation for the downward infiltration of
710 water into soil, *Water Resources Research*, *23*(5), 809-817. doi:10.1029/WR023i005p00809
711 Talsma, T., and J. Y. Parlange (1972), One-Dimensional Vertical Infiltration, *Australian Journal*
712 *of Soil Research*, *10*(2), 143-150. doi:10.1071/Sr9720143

713 Touma, J., M. Voltz, and J. Albergel (2007), Determining soil saturated hydraulic conductivity
714 and sorptivity from single ring infiltration tests, *European Journal of Soil Science*, *58*(1),
715 229-238. doi:10.1111/j.1365-2389.2006.00830.x
716 Valiantzas, J. D. (2010), New linearized two-parameter infiltration equation for direct
717 determination of conductivity and sorptivity, *Journal of Hydrology*, *384*(1-2), 1-13.
718 doi:10.1016/j.jhydrol.2009.12.049
719 van Genuchten, M. T. (1980), A closed-form equation for predicting the hydraulic conductivity
720 of unsaturated soils, *Soil Science Society of America Journal*, *44*(5), 892-898.
721 doi:10.2136/sssaj1980.03615995004400050002x
722 Vauclin, M., and R. Haverkamp (1985), Solutions quasi analytiques de l'équation d'absorption de
723 l'eau par les sols non saturés. I. - Analyse critique *Agronomie*, *5*(7), 597-606
724 Vereecken, H., et al. (2022), Soil hydrology in the Earth system, *Nature Reviews Earth &*
725 *Environment*. doi:10.1038/s43017-022-00324-6
726 White, I. (1979), Measured and Approximate Flux-Concentration Relations for Absorption of
727 Water by Soil, *Soil Science Society of America Journal*, *43*(6), 1074-1080.
728 doi:10.2136/sssaj1979.03615995004300060003x
729 Wu, S. B., T. F. M. Chui, and L. Chen (2021), Modeling slope rainfall-infiltration-runoff process
730 with shallow water table during complex rainfall patterns, *Journal of Hydrology*, *599*.
731 doi:10.1016/j.jhydrol.2021.126458
732 Wu, S. C., D. H. Ma, Z. P. Liu, J. B. Zhang, L. Chen, X. C. Pan, and L. H. Chen (2022), An
733 approximate solution to one-dimensional upward infiltration in soils for a rapid estimation of
734 soil hydraulic properties, *Journal of Hydrology*, *612*, 128188.
735 doi:10.1016/j.jhydrol.2022.128188